

Low-temperature ($\sim 250^\circ\text{C}$) route to lateral growth of ZnO nanowires

Congkang Xu, Keehan Rho, and Junghwan Chun

Department of Physics and Electron Spin Science Center, POSTECH 790-784, Republic of Korea

Dong-Eon Kim^{a)}

Department of Physics and Electron Spin Science Center, POSTECH, 790-784, Republic of Korea and Nano Device Research Center, Korea Institute of Science and Technology, Seoul 130-650, South Korea

(Received 12 July 2005; accepted 17 October 2005; published online 13 December 2005)

Zinc oxide nanowires were obtained through a vapor transport route at temperatures as low as around 250°C . The diameters of the nanowires are ~ 40 nm and their lengths reach up to a few microns. The high-resolution transmission electron microscopy showed that ZnO nanowires are of hexagonal wurtzite structures with the $[11\bar{2}0]$ growth direction. Raman spectrum reveals that the ZnO nanowires are of high-quality crystal and have an oxygen deficiency. The energy dispersive x-ray spectroscopy result verifies that the nanowires contain a small amount of Bi besides Zn and O. The investigation of the growth mechanism suggests that BiI_3 plays a key role on the fabrication of ZnO nanowires around 250°C . © 2005 American Institute of Physics.

[DOI: [10.1063/1.2142090](https://doi.org/10.1063/1.2142090)]

The nanostructure of zinc oxide has aroused great interest because of its intriguing optical functions based on its wide band-gap of 3.37 eV. A prominent feature of ZnO is its large excitonic binding energy (60 meV) at room temperature, which leads to extreme stability of excitons,¹ and enables devices to function at a low threshold voltage. Consequently, ZnO is considered a promising photonic material for the UV/blue devices such as short-wavelength light-emitting diodes and laser diodes. Recently, much attention has been paid to ZnO low-dimensional nanostructures such as nanowires and nanotubes.²⁻⁴ It also has been reported that ZnO two-dimensional (2D) and one-dimensional (1D) semiconducting nanostructures have potential applications in manufacturing short-wavelength nanolasers. A room-temperature UV nanolaser has been fabricated using ZnO nanowire arrays.⁵ To date, a variety of methods have been developed to synthesize ZnO nanostructures. For example, metalorganic vapor-phase epitaxy (MOVPE),⁶ infrared irradiation,⁷ thermal evaporation,⁸ and thermal decomposition⁹ have been used to produce aligned ZnO nanorods, tetrapodlike ZnO nanorods, and ZnO nanobelts. On the other hand, the rich defect chemistry of ZnO and its receptiveness to doping leads to a very wide range of properties including the conductivity from *n* type to *p* type,¹⁰ high transparency,¹¹ and room-temperature ferromagnetism.¹² With such a variety of functional properties, progress has been made in novel ZnO devices such as gated nano-ZnO transistors,¹³ nano-ZnO coating solid-state spinel batteries,¹⁴ and Li-ZnO optical switches.¹⁵ Most of all, the ZnO nanostructures used in these applications have been fabricated at high temperatures. The growth temperatures were not less than 400°C . Such a high temperature is disadvantageous in the fabrication of nanophotonic integrated circuits (ICs) because thermal drift¹⁶ causes inconvenience for the manipulation of size and position of nanomaterials. A low-temperature process is therefore desirable for nanostructures.

In this letter, we report the lateral growth of ZnO nanowires at a temperature as low as 250°C . These ZnO nanowires contain a small amount of Bi elements. Bi-ZnO nanowires may be used as nanovaristors in nanocircuits to protect a surge current.

Bismuth iodide (99.999%, Aldrich) and zinc (99.998%, 100 mesh, Aldrich) were mixed homogeneously in a mortar and ground using a pestle for ~ 15 min. First, the mixture was loaded into an 8-cm-long alumina boat that was then covered by three pieces of oxidized silicon substrates. The gaps between the three substrates were approximately 1 mm. Second, the covered boat was placed in the center of a quartz tube. A high-purity argon gas at a flow rate of 150 SCCM was fed into the quartz tube. The furnace was heated up to around 250°C and held at this temperature for 30 min. During this period, air was momentarily introduced into the reaction chamber through the outlet end of the furnace. After cooling down the furnace to ambient temperature, the samples were obtained from the substrates.

The morphology of as-prepared nanowires on the substrates was examined using scanning electron microscope (SEM) and JEOL-2010 high-resolution transmission electron microscopy (HRTEM) equipped with an energy dispersive x-ray spectrometry (EDX) system and Japanese Rigaku D/max γA x-ray powder diffractometer (XRD). Raman spectra were recorded at room temperature, using the Ar^+ laser line at 488 nm as an excitation source.

Figure 1(a) is the SEM image of the nanowires grown on an oxidized silicon substrate. The nanowires are very dense and distributed over an entire substrate surface area. The average diameter is about 40 nm and length a few microns. Figure 1(b) shows the magnified SEM image. There are spearlike tips on the tops of some nanowires. From SEM EDX analyses, the tip indicated by *A* is composed of Zn, O, Bi, and Si with an atomic ratio of 5.4, 49.1, 0.2, and 45.3. The atomic ratio of Zn to Bi is 97:3. The presence of Si is due to the substrate. The area indicated by *B* consists of Zn, O, and Si with an atomic ratio of 5.7, 46.6, and 47.7. The excessive oxygen in this SEM EDX is due to the contribu-

^{a)} Author to whom correspondence should be addressed; electronic mail: kimd@postech.ac.kr

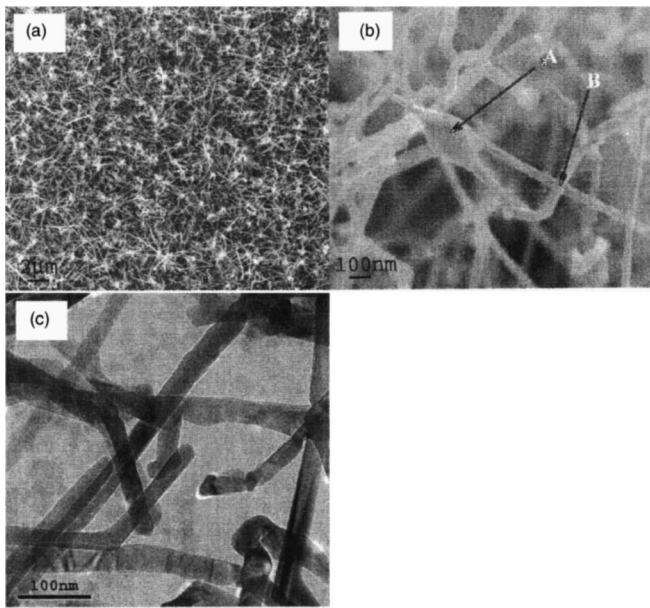


FIG. 1. (a) SEM image of the nanowires grown on an oxidized Si substrate. (b) Magnified SEM image of nanowires with spearlike tips. (c) TEM image.

tion from the oxidized Si substrate. The correct stoichiometry of ZnO is observed in TEM EDX data, as discussed below. The fact that the nanowire tip contains Bi discloses that the nanowires were dominated by the vapor-liquid-solid (VLS) mechanism, even though the growth temperature is as low as 250 °C. The TEM image is shown in Fig. 1(c), where kinks are seen and may be due to defect and/or strain from nearby neighboring nanowires. It has been reported that the close proximity of neighboring nanowires may induce the strain, forcing nanowires to change the growth direction.^{8,17}

Figure 2 illustrates the XRD. The diffraction peaks are quite similar to those of a bulk ZnO, which can be indexed as the hexagonal wurtzite structure ($a=3.18$ Å, $c=5.18$ Å). No typical diffraction peak corresponding to Bi or Bi compound impurity phases is observed.

Figure 3(a) is the TEM of a single nanowire. The diameter of the nanowire is approximately 40 nm. The lower inset is the EDX data, indicating that the nanowire consists of Zn, O, and Bi with an atomic ratio of 48.74, 51.23, and 0.03. The results reveal that a stoichiometric nanowire [(Zn+Bi)/O

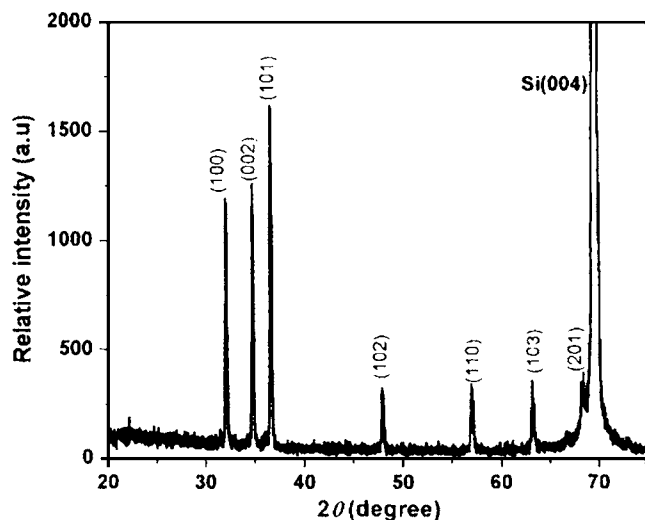


FIG. 2. XRD pattern of ZnO nanowires.

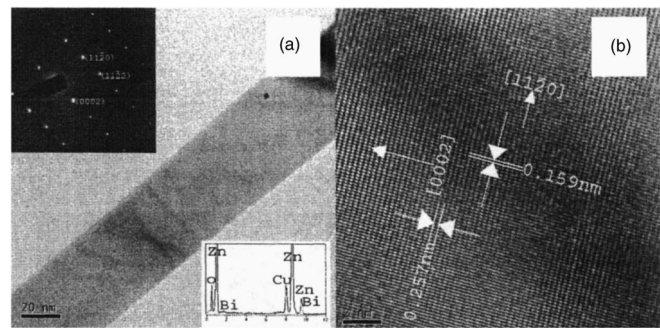


FIG. 3. (a) TEM image of a nanowire. The upper inset is SAED; the lower inset is EDX. Scale bar: 20 nm (b) HRTEM of the corresponding nanowire. Scale bar: 2 nm.

$\approx 1:1$] is obtained. The atomic ratio of Zn to Bi is 99.94:0.06. The upper inset is the selected area electron diffraction (SAED) pattern. The diffraction spots can be assigned to single crystal hexagonal wurtzite ZnO structure with a zone axis of $[1\bar{1}00]$ being consistent with the above XRD results. The nanowire grows along the $[11\bar{2}0]$ direction unlike ZnO nanowires fabricated at a high temperature without catalyst, in which ZnO nanowires grow along $[0001]$.¹⁸ Even though the Bi element has been detected by the EDX, no secondary phase is observed. Figure 3(b) is its high-resolution (HR) TEM image. The interplanar spacings of 0.257 nm and 0.159 nm correspond to (0002) and $(11\bar{2}0)$ planes, respectively.

Figure 4 shows the typical Raman spectrum excited by a 488-nm laser line. The peak at 518 cm^{-1} can be attributed to the contribution from the oxidized Si substrate. The peaks at 331, 381, 436, and 584 cm^{-1} are assigned to $E_{2H}^-E_{2L}$, A_{1T} , E_{2H} , and E_{1L} of the bulk ZnO, respectively. The E_{2H} mode involving only oxygen atoms¹⁹ articulates that the nanowires are of high-quality crystal. The E_{1L} mode is associated with oxygen deficiency,²⁰ indicating that oxygen vacancies exist in the nanowires. In comparison with Au-catalyzed ZnO nanowires,⁸ the E_{2H} mode of ZnO nanowires is shifted toward lower frequency by a small amount of 1 cm^{-1} , which may be mainly attributed to strains and defects.^{21,22}

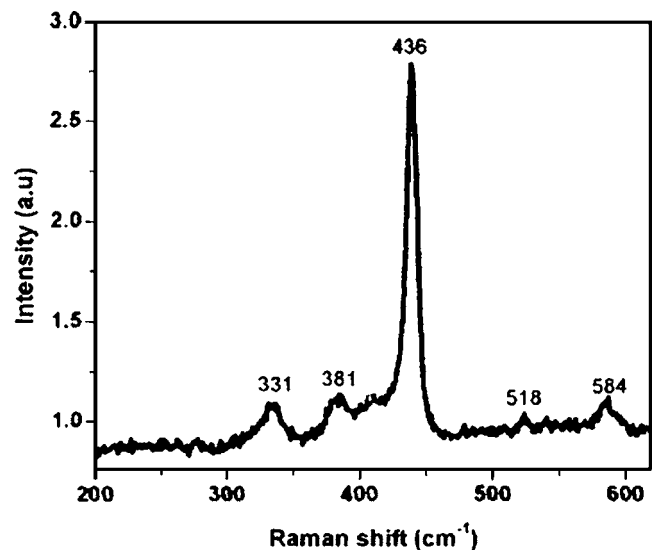


FIG. 4. Raman spectrum of ZnO nanowires grown on an oxidized Si substrate. The excitation was done by a 488-nm laser line.

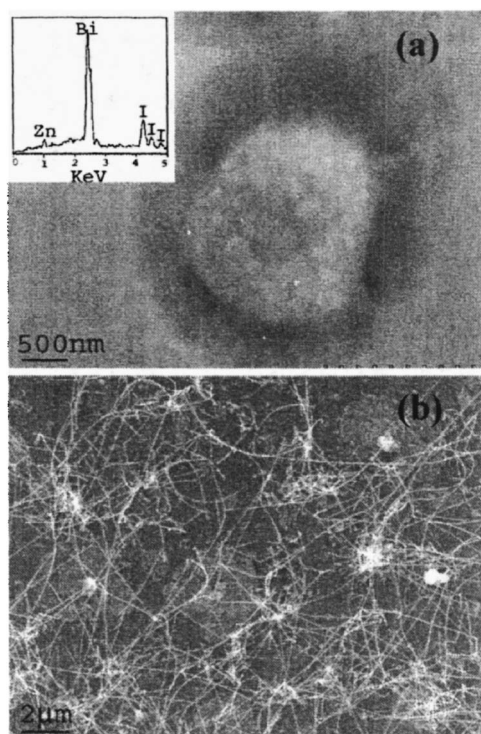


FIG. 5. (a) SEM image of as-prepared samples fabricated without the introduction of oxygen. The inset is for EDX. (b) SEM image of ZnO nanowires around 200 °C.

To know how ZnO nanowires were formed around 250 °C, a series of experiments were conducted. Major results are as follows: (i) No nanowire was obtained at a temperature lower than 400 °C in the absence of BiI₃, indicating that BiI₃ is a key factor for the low-temperature growth of ZnO nanowires. (ii) White materials were obtained without the introduction of oxygen [Fig. 5(a)]. When they were exposed to air for a while, their color became wet yellow. The EDX analysis (the inset) shows that they are composed of Zn, Bi, and I with an atomic ratio of 6.7, 42.9, and 50.4. (iii) Only a small amount of ZnO nanowires were obtained at ~200 °C [Fig. 5(b)], manifesting that sufficient liquid-phase Bi–Zn alloys were not produced below the melting point of the Bi–Zn alloy.²³ In other words, these ZnO nanowires are formed via the VLS mechanism from Bi–Zn droplets and BiI₃ plays a key role. In accordance with our experiments results, the growth processes of ZnO nanowires may be proposed as follows: (a) When the temperature rises, these reactions may occur: $3\text{Zn} + 2\text{BiI}_3 \rightarrow 3\text{ZnI}_2 + 2\text{Bi}$, $2\text{BiI}_3 \rightarrow 2\text{Bi} + 3\text{I}_2$. (b) According to Bi–Zn phase diagram,²³ the mixture of Bi and Zn can form a liquid phase at 254.5 °C. (c) Bi–Zn droplets can be carried away and subsequently deposited on the substrate. (d) When air is introduced into the furnace, ZnO is formed. Since ZnO is not soluble in the liquid phase, ZnO precipitates and leads to the growth of a crystalline nanowire on substrate. This growth mechanism indicates that the growth of ZnO nanowires is associated with and affected by ZnI₂ (tetragonal layered structure) and BiI₃ (hexagonal layered structure). This may explain the observation of the different growth direction of the nanowire in our case. In

other words, the predeposited layered structure suppresses the growth of the ZnO nanowire in the [0001] direction but allows the growth in the [11 $\bar{2}$ 0] direction.

In summary, ZnO nanowires were obtained through a vapor transport route at a temperature of around 250 °C. Their diameters are ~40 nm and lengths reach up to a few microns. HRTEM shows that ZnO nanowires are of hexagonal wurtzite structures and grow along the [11 $\bar{2}$ 0] direction. Raman spectrum indicates that the ZnO nanowires are of high-quality crystal and oxygen deficiency. EDX verifies that the nanowires contain a small amount of bismuth besides Zn and O. The study of the growth mechanism shows that BiI₃ plays a key role on the achievement of ZnO nanowires around 250 °C. This method offers a new approach to the fabrication of ZnO nanowires at a low temperature. These ZnO containing Bi nanowires may have important applications in nanovaristors to protect a surge current.

This work was supported by electron Spin Science Center (eSSC), and in part by National Research Laboratory Project funded by Korean Science and Engineering Foundation (KOSEF).

- ¹Y. Chen, D. M. Bagnall, H. Koh, K. Park, K. Hiraga, Z. Zhu, and T. Yao, *J. Appl. Phys.* **84**, 3912 (1998).
- ²Z. W. Pan, Z. R. Dai, and Z. L. Wang, *Science* **291**, 1947 (2001).
- ³J. Wu and S. Liu, *Adv. Mater. (Weinheim, Ger.)* **14**, 215 (2002).
- ⁴C. K. Xu, M. Kim, J. Chun, and D. E. Kim, *Nanotechnology* **16**, 2104 (2005).
- ⁵M. H. Huang, S. Mao, H. Feik, H. Yan, Y. Wu, H. Kind, E. Weber, R. Russo, and P. Yang, *Science* **292**, 1897 (2001).
- ⁶W. I. Park, D. H. Kim, S. W. Jung, and G. C. Yia, *Appl. Phys. Lett.* **80**, 2002 (4232).
- ⁷Y. B. Li, Y. Bando, T. Sato, and K. Kurashima, *Appl. Phys. Lett.* **81**, 144 (2002).
- ⁸X. Wang, Q. Li, Z. Liu, J. Zhang, and Z. Liu, and R. Wang, *Appl. Phys. Lett.* **84**, 4941 (2004).
- ⁹C. Xu, G. Xu, Y. Liu, and G. Wang, *Solid State Commun.* **122**, 175 (2002).
- ¹⁰M. Joseph, H. Tabata, and T. Kawai, *Jpn. J. Appl. Phys., Part 2* **38**, L1205 (1999).
- ¹¹T. Minami, H. Sato, H. Imamoto, and S. Takata, *Jpn. J. Appl. Phys., Part 2* **31**, L257 (1992).
- ¹²K. Ueda, H. Tabata, and T. Kawai, *Appl. Phys. Lett.* **79**, 988 (2002).
- ¹³A. L. Roest, J. J. Kelly, D. Vanmaekelbergh, and E. A. Meulenkaamp, *Phys. Rev. Lett.* **89**, 036801 (2002).
- ¹⁴Y. K. Sun, K. J. Hong, J. Prakash, and K. Amine, *Electrochem. Commun.* **4**, 344 (2002).
- ¹⁵T. Nagata, T. Shimura, A. Ashida, N. Fujimura, and T. Ito, *J. Cryst. Growth* **237–239**, 533 (2002).
- ¹⁶M. Ohtsu, K. Kobayashi, T. Kawazoe, S. Sangu, and T. Yatsui, *IEEE J. Sel. Top. Quantum Electron.* **8**, 839 (2002).
- ¹⁷Z. H. Wu, X. Mei, D. Kim, M. Blumin, and H. E. Ruda, *Appl. Phys. Lett.* **83**, 3368 (2003).
- ¹⁸C. K. Xu, M. Kim, S. Chung, and D. E. Kim, *Solid State Commun.* **132**, 837 (2004).
- ¹⁹S. K. Sharma and G. J. Exarhos, *Solid State Phenom.* **55**, 32 (1997).
- ²⁰J. J. Wu and S. C. Liu, *J. Phys. Chem. B* **106**, 9546 (2002).
- ²¹Y. Huang, M. Liu, Z. Li, Y. Zeng, and S. Liu, *Mater. Sci. Eng., B* **97**, 116 (2003).
- ²²C. K. Xu, S. Chung, M. Kim, D. E. Kim, B. Chon, S. Hong, and T. Joo, *J. Nanosci. Nanotechnol.* **5**, 530 (2005).
- ²³H. Yumato, T. Kaneko, R. R. Hasiguti, and T. Watanabe, *J. Cryst. Growth* **84**, 185 (1987).